JMEPEG (2010) 19:274–281
DOI: 10.1007/s11665-009-9441-7

1059-9495/$19.00

Pitting and Intergranular Corrosion Resistance of AISI Type 301LN Stainless Steels

S. Ningshen and U. Kamachi Mudali

(Submitted June 25, 2008; in revised form March 18, 2009)

The pitting and intergranular corrosion (IGC) resistance of AISI type 301LN stainless steels were evaluated using ASTM methods, anodic polarization, and electrochemical impedance techniques. The IGC results indicated that the microstructure of the samples after sensitization heat treatment at 675 °C for 1 h shows step or dual structure for both imported and indigenous materials indicating insignificant $Cr_{23}C_6$ precipitation. The results of immersion tests in boiling 6% copper sulfate + 16% sulfuric acid + copper solution for 24 h followed by the bend test (ASTM A262 Practice-E method) indicated no crack formation in any of the tested specimens. Pitting corrosion resistance carried out in 6% $FeCl_3$ solution at different temperatures of 22 ± 2 and 50 ± 2 °C (ASTM G 48) up to the period of 72 h revealed pitting corrosion attack in all the investigated alloys. The potentiodynamic anodic polarization results in 0.5 M NaCl revealed variation in passive current density and pitting potential depending on the alloy chemistry and metallurgical condition. The passive film properties studied by electrochemical impedance spectroscopy (EIS) correlated well with the polarization results. The x-ray diffraction (XRD) results revealed the presence of austenite (γ) and martensite (α′) phases depending on the material condition. The suitability of three indigenously developed AISI type 301LN stainless steels were compared with imported type 301LN stainless steel and the results are highlighted in this article.

Keywords intergranular corrosion, nitrogen and passive film, pitting

1. Introduction

Austenitic stainless steels are widely used in various engineering applications such as chemical, petrochemical, fertilizer, and nuclear industries because of good combination of high strength, formability, weldability, and corrosion resistance (Ref 1-5). Mass transit systems all over the world are turning to austenitic metastable stainless steel for railcars to reduce weight, provide high strength and impact safety, and minimize the higher costs for corrosion protection and life-cycle costs (Ref 6-10). AISI type 301 stainless steels characterized by a metastable structure are fully austenitic (γ-phase) in annealed condition but partially transform to martensite during deformation (Ref 6-8). In the annealed state, these steels show low yield strength (300 MPa); however, significant strengthening (1500 MPa) can be achieved by cold plastic deformation (Ref 8-10). Furthermore, addition of N provides higher volume fractions of martensite during cold rolling and, consequently, form smaller austenite grains on annealing (Ref 9, 10). This transformation affects the mechanical properties significantly, from large ductility after annealing to high strength after cold rolling (Ref 8, 11). Such an effect is an essential requisite for structural parts where resistance and torsional rigidity are necessary in applications including railcars and automobile industries. Railcar bodies made of AISI type 301LN (16Cr-7Ni-0.15N) austenitic stainless steel weigh less than 55% compared to bodies made of carbon steel, and is currently used in Japanese commuter trains (Ref 8) and in Delhi metro railway mass transport system in India (Ref 9). AISI type 301LN austenitic stainless steel which contains lower Cr and Ni contents than 304L or 316L stainless steel has economic merit compared to other austenitic stainless steels (Ref 9-14). However, pitting corrosion, and sensitization leading to intergranular corrosion (IGC), can be associated with the application of type 301LN stainless steel to be used in mass transit railcar industries (Ref 12, 14).

The scope of this work is to evaluate the pitting corrosion and IGC resistance of different AISI type 301LN stainless steels to be used for mass transit railcars. The phase changes induced by cold working and annealed conditions and its effect on the corrosion resistance are discussed and highlighted in this article.

2. Materials and Experimental Work

The chemical compositions of four different AISI type 301LN stainless steel used in this investigation are given in Table 1. AISI type 301LN stainless steel used in this investigation was designated as 301LN-1 (imported), 301LN-2 (30% cold work), 301LN-3, and 301LN-4. Solution annealing treatment was carried out for 301LN-1, 301LN-2, and 301LN-4 stainless steel, and 301LN-3 was obtained in full hard condition followed by solution annealing. All indigenously developed AISI type 301LN stainless steels used in this investigation were supplied by Steel Authority of India Limited (SAIL), Salem Steel Plant, Salem, India.

S. Ningshen and **U. Kamachi Mudali**, Corrosion Science and Technology Division, Indira Gandhi Centre for Atomic Research, Kalpakkam 603 102, India. Contact e-mail: kamachi@igcar.gov.in.

Table 1 Chemical compositions of AISI type 301LN stainless steels (wt.%)

Alloy	Cr	Ni	Mn	C	N	Si	S	P
301LN-1	17.26	6.53	1.58	0.019	0.10	0.55	0.003	0.173
301LN-2	16.96	6.61	1.56	0.017	0.146	0.62	0.003	0.034
301LN-3	16.89	6.66	1.70	0.016	0.166	0.42	0.001	0.018
301LN-4	16.90	7.10	1.64	0.020	0.173	0.44	0.003	0.033

2.1 Specimen Preparation

The as-received stainless steel plate was cut into 10 mm × 10 mm size specimens. All the specimens were then polished up to 600 grit using SiC paper and then mounted in epoxy resin (araldite). The samples were then polished up to 1 μm diamond finish for further corrosion studies.

2.2 Microstructure and IGC Evaluation

IGC evaluation caused by sensitization was carried out in accordance with ASTM A262 Practice tests (Ref 15). All the samples used in this study were given a sensitization heat treatment at 675 °C for 1 h (ASTM-A262) prior to Practice A and E tests. To classify the microstructures, all the stainless steel samples were electrolytically etched at 1 A/cm^2 for 1.5 min using 10% oxalic acid. The etched structure was examined in optical microscopy and was characterized as step, dual, or ditch structure.

ASTM A262 Practice E test was carried out by immersion and boiling of specimen for 24 h in copper + 6% copper sulfate + 16% sulfuric acid solution (Ref 15). Subsequently, the bend test was carried out holding the tested specimen in vise and bend over a diameter equal to the thickness of the specimen (or bent through 180°). If cracks were observed, the material was considered to be sensitized.

2.3 Pitting Corrosion Evaluation Using 6% $FeCl_3$ Solution

The relative pitting corrosion evaluations were carried out using 6% $FeCl_3$ solution (Ref 16). The specimens were placed in a glass cradle and immersed in the test solution at two different temperatures of 22 ± 2 and 50 ± 2 °C up to 72 h. After the test, the specimens were removed, rinsed with water, dipped in acetone, and air dried. The weight of each specimen was taken and the specimens were observed under microscopy for pitting corrosion morphology.

2.3.1 Pitting Corrosion Studies Using Potentiodynamic Polarization Test Method. Pitting corrosion studies were carried out in 0.5 M NaCl solution at room temperature using potentiodynamic polarization technique. The electrode potential was anodically scanned at a rate of 10 mV/min from −500 mV till pitting corrosion occurred. The potential at which a monotonic increase in the anodic current exceeds 25 μA was termed as the critical pitting potential (E_{pp}). All the electrode potentials were measured with respect to saturated Ag/AgCl reference electrode. Three to four sets of pitting corrosion tests were conducted for each specimen. The electrolyte was continuously purged with purified argon to deaerate the solution till the end of experiment. Details of the experimental methods have been already describes elsewhere (Ref 17, 18).

2.3.2 Electrochemical Impedance Spectroscopy Studies. Electrochemical impedance spectroscopy (EIS) measurements were carried out using Solartron 1255 Frequency Response Analyzer (FRA) and Solartron 1287 Electrochemical Interface. The experiments were carried out in the frequency range of 0.01 Hz to 100 kHz by superimposing an AC voltage of 10 mV amplitude at open circuit potential. The EIS results were interpreted using "equivalent circuit" shown in Fig. 1. The circuit description consists of the arrangement of [R_s(CPE||R_P)] elements, where R_s is the solution resistance and CPE is the constant phase in parallel connection with R_P which is the polarization resistance at the interface. The characteristic parameter values of these elements are then obtained directly by fitting the experimental impedance curves using Zview Version 2.6 (Scribner Inc.) software.

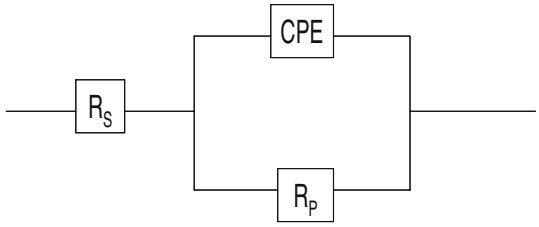

Fig. 1 The equivalent circuit (R_S[CPE||R_P]) used for the fitting the experimental Nyquist impedance plots

The impedance expression of CPE (Ref 19) is given by $Z_{CPE} = 1/[T(j\omega)^n]$, where ω is the angular frequency, T and n are frequency-independent fit parameters, $j = (-1)^{1/2}$, and $\omega = 2\pi f$, where f is the frequency (Hz). CPE has been used in this investigation to obtain better fit for experimental data and this will represent generalized form of passive film double layer capacitance. EIS measurements under same condition are almost reproducible.

2.3.3 X-Ray Diffraction Analysis. The XRD analysis was performed on the alloy samples by using INEL Model x-ray 300 diffractometer. Diffraction lines were recorded in the range of 2θ = 20° to 100° by applying filtered cobalt radiation (λKα = 1.78892 Å).

3. Results and Discussion

3.1 XRD Pattern of Type 301LN Stainless Steels

The XRD patterns of type 301LN stainless steels in solution annealed (301LN-1 and 301LN-4), as cold rolled (301LN-2), and full hard plus solution annealed (301LN-3) and its constituent phases are shown in Fig. 2(a) to (d), respectively. The results of diffraction patterns of phase analysis revealed the presence of austenite (γ-phase) and α′-martensite depending on the material condition. In solution-annealed type 301LN-1 stainless steel (Fig. 3a), the XRD pattern is typical of austenite γ-phase, the peaks of which appear at 2θ = 45.67°, 50.80°, 91.68°, and so on, with traces of α′-martensite (43.65°, 51.3°, and 82.85°). In 301LN-2 stainless steel, the XRD pattern of as-deformed sample shown in Fig. 2(b) reveals the presence of

the α′-martensite (2θ = 43.65°, 74.68°, and 95.27°) induced by cold rolling. Similarly, in full hard and solution-annealed sample of 301LN-3 stainless steel shown in Fig. 2(c), γ-austenite peak (45.65°, 64.57°, and 91.74°) with certain amount of α′-martensite (43.65°, 83.21°) is observed. Metastable type 301LN stainless steels are susceptible to a deformation-induced martensitic transformation and can alter the mechanical and corrosion properties (Ref 6, 8, 10, 20). Furthermore, in austenitic steels, the γ → α′ transformation rate increases with increase in the degree of deformation (Ref 21). Other factors that affect the strain-induced phase transformation are the strain rate, grain size, and deformation mode (stress state) (Ref 12, 20). The most important are the alloy chemical composition and the temperature at which the plastic deformation takes place (Ref 22). It has been observed that increase in Cr and N suppresses such transformation and Ni and C are known to have strong opposite effect (Ref 22, 23). During martensitic transformation, α′-martensite is nucleated in the austenite phase at the intersections of shear bands that consist of stacking fault bundles and mechanical twins (Ref 24). In this study, no evidence of the presence of ε-martensite was found in the XRD pattern. Therefore, all the samples were considered to contain only γ-austenite and marginal α′-martensite phases depending on the alloy condition.

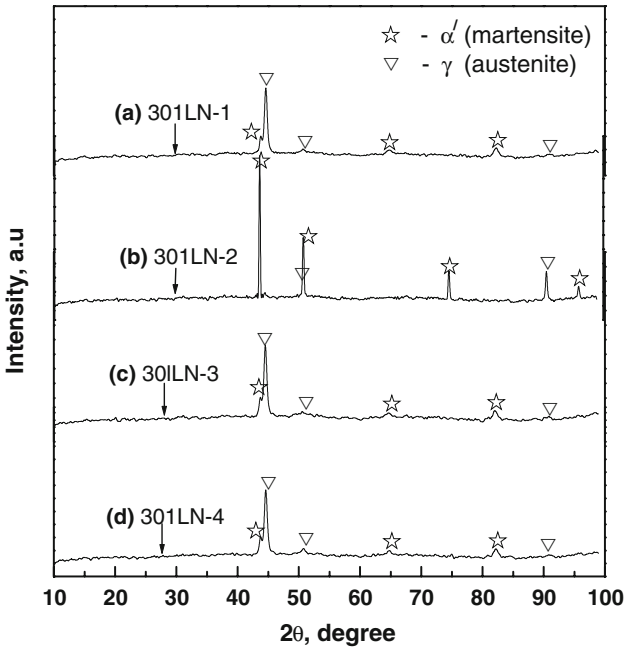

Fig. 2 XRD patterns of different AISI type 301LN SS

3.2 Intergranular Corrosion Resistance

The microstructural evolution of different type 301LN stainless steels in soft (solution annealed), cold rolled, and full hard conditions has been studied. The IGC due to sensitized microstructure is one of the major problems faced by austenitic stainless steel components used in various industries (Ref 3, 25, 26). The formation of such precipitates comprising Cr-rich $M_{23}C_6$ carbide (M = Cr, Ni, Fe; Cr-65 wt.%, Ni-10 wt.%, and Fe-5 wt.%) or Cr_2N at grain boundaries during heat treatment (from 450 to 750 °C), welding, fabrication, or irradiation restricts their use in aqueous environments (Ref 3, 26). The results of the electrochemically etched microstructure of different type 301LN stainless steels are shown in Fig. 3(a) to (d). The microstructure of all the tested samples showed mostly

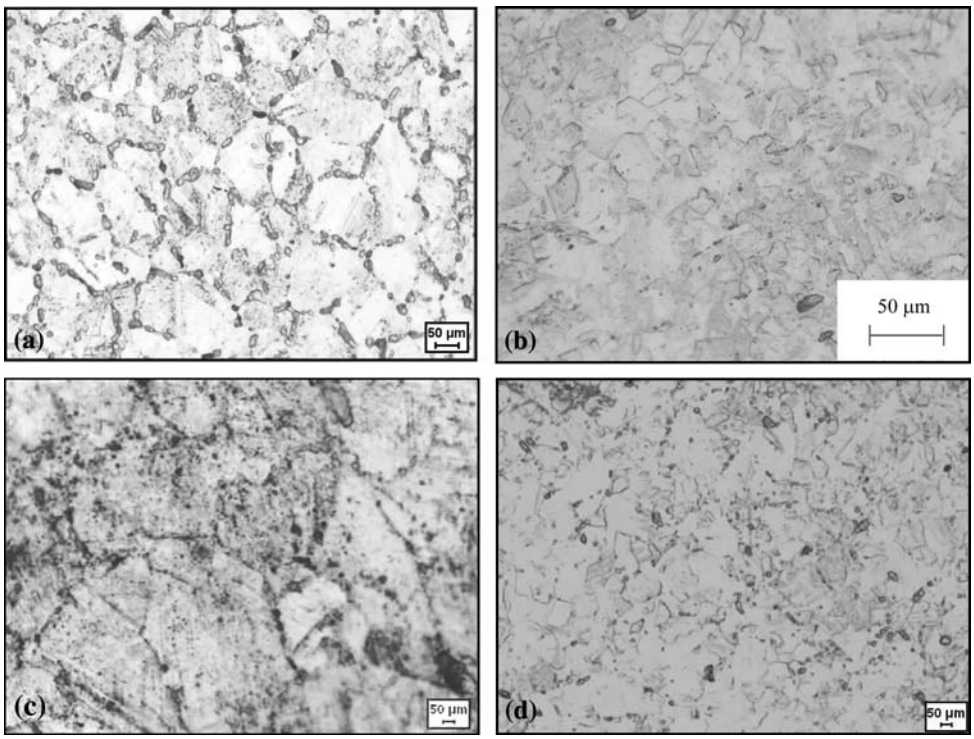

Fig. 3 Optical micrographs of different AISI type 301LN stainless steels etched using 10% oxalic acid after heat treatment at 675 °C for 1 h: (a) 301LN-1, (b) 301LN-2, (c) 301LN-3, and (d) 301LN-4

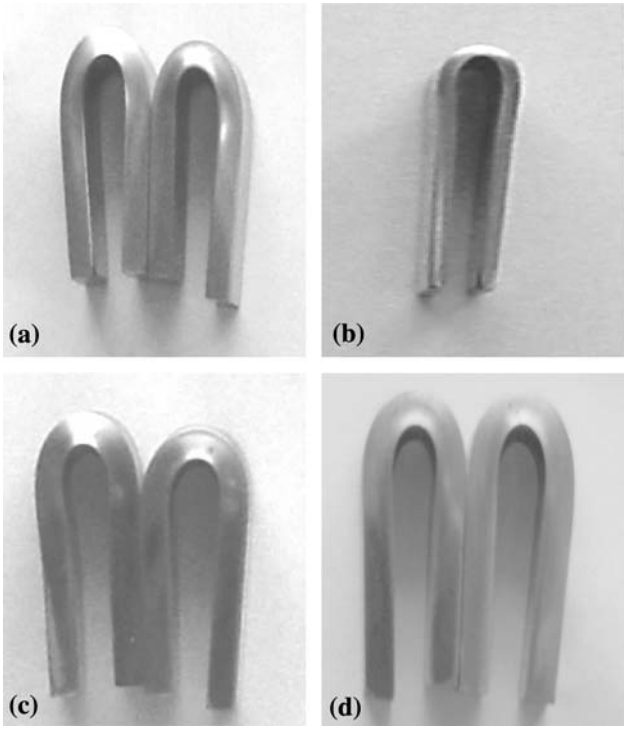

Fig. 4 Bend test for IGC evaluation of different type 301LN stainless steels after boiling for 24 h in copper + 6% copper sulfate + 16% sulfuric acid solution (ASTM-A262 Practice E): (a) 301LN-1, (b) 301LN-2, (c) 301LN-3, and (d) 301LN-4

dual and scattered carbide precipitates throughout the structure. The martensitic formation in cold-rolled sample (301LN-2) was confirmed by XRD analysis (Fig. 2), and the formation of fine austenite grains was observed in type 301LN-3 stainless steel (Fig. 3c).

The results of bend test carried out after exposure of specimens to copper + 6% copper sulfate + 16% sulfuric acid solution for 24 h to assess the IGC resistance of type 301LN stainless steel are shown in Fig. 4(a) to (d). It is clearly observed from these photo macrographs that all the investigated alloys after the bend test did not show crack formation, indicating that the specimen is unaffected by sensitization heat treatment (675 °C for 1 h). These results clearly revealed that AISI type 301LN stainless steel in different metallurgical condition showed good resistance to sensitization. In stainless steel, C and N play predominant role in controlling sensitization kinetics. The tendency for sensitization and intragranular precipitation increases with the increasing C content in the alloy, and the addition of N offsets deleterious effect of C (Ref 3, 25, 26).The detrimental effect of C on sensitization can be further reduced by the addition of stabilizing elements like Ti and Nb. Strong carbide-forming elements such as Nb and Ti preferentially combine with the available C and lessen the opportunity for $Cr_{23}C_6$ to nucleate (Ref 26, 27). Similarly, alloys with higher Cr contents are more resistant to sensitization as time to Cr depletion at the grain boundaries is shifted to longer duration (Ref 28). The beneficial effects of N on the sensitization have been observed in many studies (Ref 3, 14, 25, 26, 29), and the retardation of sensitization by N has been confirmed for alloys with N up to 0.16 wt.% (Ref 27, 28). In the present alloys, subsequent to $Cr_{23}C_6$ precipitation, the grain

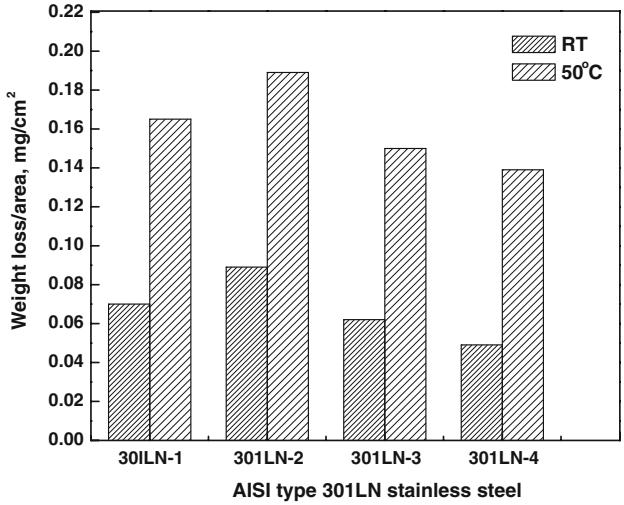

Fig. 5 Weight loss changes in 6% $FeCl_3 \cdot 6H_2O$ after 24 h immersion for type 301LN SS

boundary Cr depletion can be delayed by the presence of N. Nitrogen is known to retard the nucleation and growth of $Cr_{23}C_6$ precipitation and changes the activity of Cr in equilibrium with the carbide (Ref 26-29). However, the details of kinetics of precipitation are not yet fully understood. Moreover, IGC arising due to sensitizing also depends on various other factors like alloy composition, grain size, cold work, heating/cooling rates, heat-treating temperature, and time (Ref 3, 25, 27, 29). The key alloying element responsible for sensitization is C. Increasing N, Mn, Cr, and Mo contents are known to improve the resistance to sensitization and IGC (Ref 25, 27, 29). The negligible carbide precipitates observed in these alloys can thus be attributed to the presence of low C and higher N that delay the onset of $Cr_{23}C_6$ precipitates.

3.3 Ferric Chloride Immersion Tests

The results of the immersion test of the samples in a 6% $FeCl_3$ solution after 72 h are shown in Fig. 5. It was observed that the as-deformed cold-rolled specimen (301LN-2) showed the highest weight loss in both temperatures at 22 and 50 °C. Type 301LN-4 stainless steel with the highest N (0.173%) content showed lower weight loss at both 22 and 50 °C. As expected, the weight losses are significant at higher temperature (50 °C) compared to measurement at 22 °C. This can be attributed to the accelerated corrosion reaction at higher temperature and also due to high oxidizing and high acidic ($pH \approx 1.2$) nature of the testing solution. Compared to as-rolled cold-worked steel, solution annealed and full hard material plus annealing showed improved corrosion resistance due to decrease in the martensite content (Ref 30). Higher weight loss observed in cold-worked sample of type 301LN-2 stainless steel could be attributed to two effects: the high density of defects produced during plastic deformation that introduced defective passive film and the presence of strain-induced martensite in the structure that leads to a creation of a galvanic effect between the martensite and austenite phases (Ref 21, 30). Hence, the presence of strain-induced martensite is the main factor for reduced corrosion resistance of cold-rolled type 301LN stainless steel. Also, the defect density of the austenite and martensite phases is known to increase with increasing cold-rolling reduction (Ref 30). Thus, lower weight loss

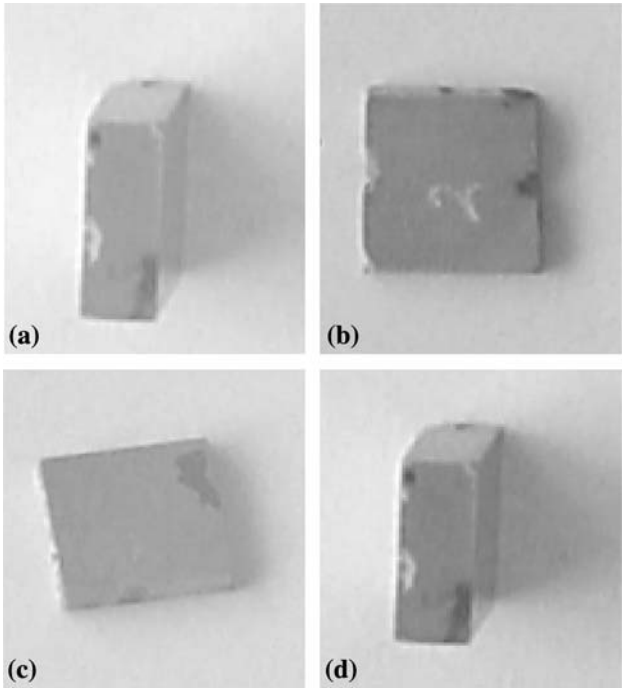

Fig. 6 Pitting corrosion resistance evaluation of AISI type 301LN stainless steels using ASTM G48 test method to the period of 72 h carried out at room temperature: (a) 301LN-1, (b) 301LN-2, (c) 301LN-3, and (d) 301LN-4

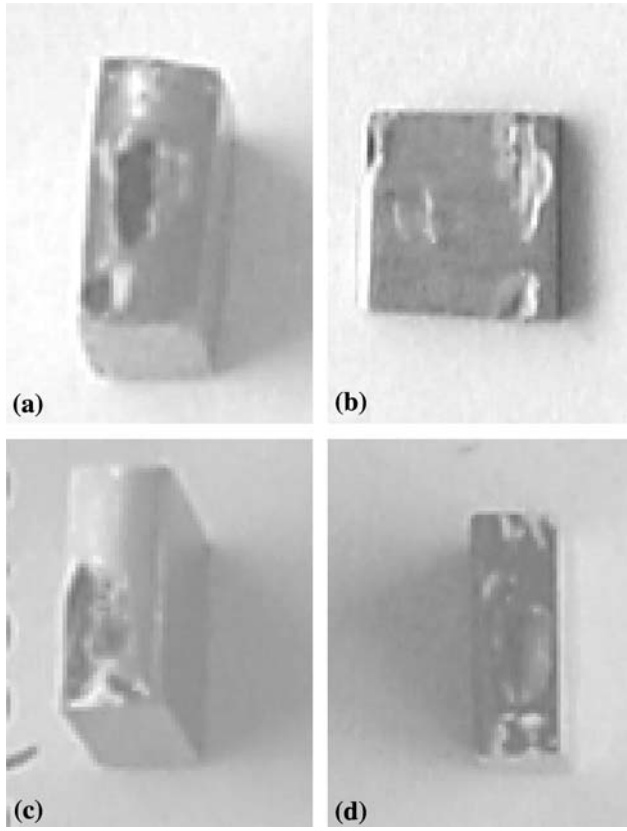

Fig. 7 Pitting corrosion resistance evaluation of AISI type 301LN stainless steels using 6% $FeCl_3$ (ASTM G48) to the period of 72 h carried out at 50 °C: (a) 301LN-1, (b) 301LN-2, (c) 301LN-3, and (d) 301LN-4

observed in type 301LN-4 stainless steel could be attributed to solution annealing and higher N content of the alloy. The solution annealing treatment resulting in reduces propensity for corrosion and increase in N are known to further improve the corrosion resistance (Ref 1, 2, 30).

The results of macrographic examination after immersion in 6% $FeCl_3$ solution in both 22 and 50 °C for 72 h indicated pitting attack in all the alloys (Fig. 6a-d and 7a-d). However, no corrosion product formation on the surface could be observed. In room-temperature studies, the photomicrograph of different samples after immersion test in 6% $FeCl_3$ indicated pitting corrosion attack (Fig. 6a-d). The cross-sectional shapes of most of the alloys showed wide and deep corrosion pit with annular in shapes. Similarly, the photomicrographs after immersion test in 50 °C (Fig. 6a-d) indicated severe pitting corrosion attack in all the specimens; pits are shallower with irregular shape of varying diameters in the range of 0.2 to 0.5 mm. The overall pit morphologies were almost similar to those specimens tested at room temperature, and the intensity of pitting attack was more at higher temperature. These results indicated that all the investigated type 301LN stainless steels are susceptible to pitting corrosion under accelerated 6% $FeCl_3$ test condition.

3.4 Potentiodynamic Anodic Polarization Studies

The results of potentiodynamic anodic polarization of type 301LN stainless steels obtained at room temperature in 0.5 M NaCl solution are shown in Fig. 8. All the potentiodynamic polarization results shown in Fig. 8 were fairly reproducible and different polarization parameters are shown in Table 2. The general shapes of the potentiodynamic curves are similar, but some differences in the corrosion potential (E_{Corr}), corrosion current density (I_{Corr}), and passive current density (I_P) could be

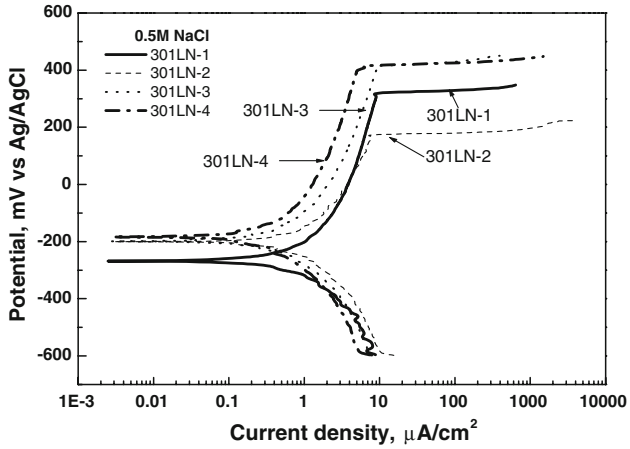

Fig. 8 Potentiodynamic anodic polarization curves of type 301LN stainless steels in 0.5 M NaCl solution

observed. However, no characteristic trend in E_{Corr} could be observed, and the differences in E_{Corr} values between the alloys are insignificant (Table 2). Passive current density (I_{Pass}) was the lowest for 301LN-4 (2.48 μA/cm^2), followed by 301LN-3 (4.2 μA/cm^2), 301LN-1 (6.06 μA/cm^2), and 301LN-2 (7.4 μA/cm^2). Almost a similar trend could be observed in I_{Corr} in the alloys. In general, I_{Pass} is a measure of the anodic dissolution or reaction rate at a certain potential in the passive region and it

Table 2 Potentiodynamic polarization parameters of 301LN stainless steels in 0.5 M NaCl solution (I_{Pass} were measured at 150 mV)

Materials	E_{Corr}, mV	I_{Corr}, μA/cm^2	I_{Pass}, μA/cm^2	E_{PP}, mV
301LN-1	−260	0.182	6.03	330
301LN-2	−190	0.168	7.36	180
301LN-3	−202	0.160	4.21	420
301LN-4	−150	0.147	2.48	430

can be used as a measure of the resistance against electrochemical corrosion. Lower I_{Pass} in higher N-containing alloy of type 301LN-4 stainless steel (0.173%N) is associated with decrease in anodic dissolution due to N addition. As observed in Fig. 8, the pitting potentials (E_{PP}) of 301LN-4 (430 mV) and 301LN-3 (420 mV) were similar and higher as compared to 301LN-1 (330 mV). Cold-worked 301LN-2 (180 mV) sample showed the lowest pitting potential. Better pitting corrosion resistance observed in solution-annealed 301LN-4 sample was due to higher N content, homogenous austenite microstructure, and dissolution of precipitates by solution annealing. Hamada et al. (Ref 30) had reported a similar results in type 301LN stainless steels, indicating reduction in the corrosion resistance by cold working in an acidic chloride solution (pH ≈ 1), but on annealing it gets improved. This was attributed to evolution of novel microstructures of retained austenite and submicron-grained austenite by annealing of cold-rolled strips.

The pitting corrosion resistance of stainless steels can be significantly affected by metallurgical variables such as cold working, alloy composition, inclusions, heat treatment, sensitization, precipitates, etc. (Ref 1-4, 25, 27). As mentioned earlier, metastable stainless steels such as type 301LN are fully austenitic (γ-phase, face-centered cubic) in annealed condition, but partially transform to martensite during deformation and this affects the corrosion resistance significantly (Ref 11). Accordingly, when the austenite transforms into the deformation-induced martensite, the number of atoms in the lattice is decreased, followed by increase in the volume with the total number of atoms unchanged (Ref 31). Thus, higher pitting corrosion resistance observed for 301LN-3 can also be attributed to the alloy chemistry and presence of higher N content (0.166%). The reduction in pitting corrosion resistance of type 301LN-2 stainless steel (180 mV) may be attributed to defect density introduced by cold rolling. The detrimental effects of deformation substructure defects affecting the corrosion resistance in austenitic stainless steel have been reported in a number of studies (Ref 6, 10, 32-35). Elayaperumal et al. (Ref 35) observed increase of the passivation current density with deformation in AISI type 304 stainless steel due to strain-induced martensite in the structure. Similarly, Barbucci et al. (Ref 6) observed a detrimental effect of the strain-induced martensite phase on the corrosion resistance of AISI type 301 stainless steel in 1 M H_2SO_4.

In this work, formation of strain-induced martensite has been conformed in cold-worked type 301LN-2 stainless steel (Fig. 2). It has been reported that martensite formed after deformation is more negative in the galvanic potential series and thus affects the corrosion behavior (Ref 36). Similarly, Sunada et al. (Ref 37) have reported the direct correlation between pitting corrosion resistance and martensite content in AISI type 304 SS. It is evident from this work that the annealing treatment of AISI type 301LN stainless steel reduces the propensity for localized corrosion. Furthermore, by comparing the pitting corrosion resistance of the investigated alloys, it is observed that the pitting corrosion resistances of indigenous (301LN-3 and 301LN-4) stainless steels are better or comparable to the imported material (301LN-1). Except in cold-worked specimen (301LN 2), the pitting corrosion resistance was lower compared to imported material. However, due to varying and scattered chemical composition in the present investigated alloys, the specific role of N cannot be differentiated; however, it demonstrates that higher N content enhanced the pitting corrosion resistance. Higher N content increasing the pitting corrosion resistance in austenitic stainless steels has been observed in many of our earlier works (Ref 2, 17, 18, 25, 34). The beneficial effect of N in improving the pitting corrosion resistance is well known and numbers of proposals have been suggested toward the role of N (Ref 1-5). These include the local buffering effect of N by formation of either NH_3, NH_4^+, NO_3^+, nitride, etc., N impending active dissolution, enrichment in passive film, barrier layer, N-Mo synergism, N retarding $Cr_{23}C_6$ precipitation, ferrite and deformation-induced α′ and ε, etc. (Ref 1-5, 10, 17, 26-28, 38, 39). However, based on the above observation, it can be summarized that the indigenously developed type 301LN stainless steel possesses better corrosion resistance compared to imported grade in chloride environment.

3.5 EIS Studies

The EIS results of type 301LN stainless steel measured under open circuit potential (OCP) in deaerated 0.5 M NaCl solution are displayed in Fig. 9. The EIS results of the Nyquist plot showed an unfinished single semicircle arc, and distinct differences can be observed in all the impedance spectra depending on the condition of the samples (Fig. 9). In general, the increase in semicircle arc radius is normally indicated by the increase in R_p value which is inversely proportional to the corrosion rate of the system. All the fitting parameters of the impedance plots are given in Table 3, both as capacitance CPE-T, the correspondent CPE power 'n' and polarization resistance R_P. The simulated curves basically follow the experimental data for most of the measurements.

When a protective passive oxide film is formed on the metal surface, the obtained impedance corresponds mainly to the

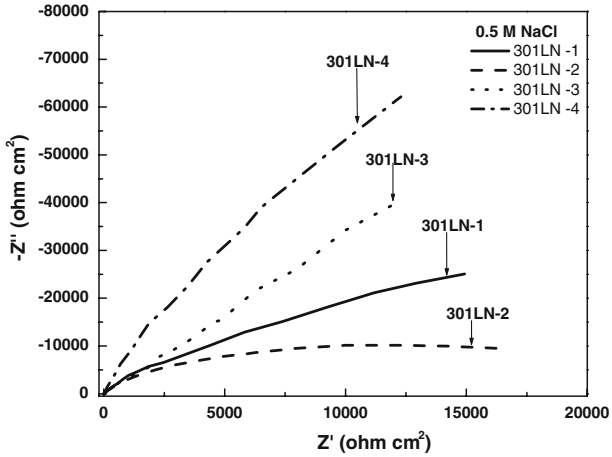

Fig. 9 EIS measurement of AISI type 301LN stainless steels in 0.5 M NaCl solution

Table 3 EIS-fitted value of AISI type 301LN stainless steels in 0.5 M NaCl solution

Alloys	R_s, $\Omega \cdot cm^2$	CPE-T, $F/cm^2\ s^{-n}$	CPE-n	R_p, $\Omega \cdot cm^2$
301LN-1	1.7	6.25×10^{-5}	0.961	17292
301LN-2	1.3	5.08×10^{-5}	0.892	16331
301LN-3	1.4	2.76×10^{-5}	0.844	15953
301LN-4	2.9	8.72×10^{-5}	0.935	20253

impedance of surface passive film as the metal's charge transfer reaction is relatively small (Ref 10, 19). Thus, the stability of passive films and its corrosion resistance is determined by the alloy composition, electrolyte media, and condition of the material (Ref 2, 18, 25). Also, the changes in the passive film properties are attributed to structural changes in the film and changes in the ionic or electrical conductivity of the passive film (Ref 38, 39). In Table 3, higher R_P values are observed for type 304L-4 stainless steel followed by alloy 301LN-3 and 301LN-1, except for the as-rolled type 301LN-2 stainless steel, the R_P value is lower. R_P values are strongly dependent on the passive film characteristic and are a measure of corrosion resistance of the materials. The higher R_P value implies good corrosion resistance, and lower value could indicate the interaction of underlying metal with electrolyte solution accelerating the oxidation and corrosion of the metal. Based on electrochemical impedance spectra observation, higher R_P measurements indicating higher corrosion resistance are consistent to passive current density and pitting potential of the investigated alloys. Lower R_P values observed in type 301LN-2 stainless steel may be related to increase in ionic conductivity through the passive film or thinning of passive film resulting in nonprotective passive film (Ref 19, 36). CPE-T is a measure of generalized capacitance of the interface to store charge corresponding to the space charge region developed in the oxide near the film/electrolyte interface (Ref 19, 36). CPE-T changes can be affected by the presence of adsorbed anions or surface compositions. The relatively higher CPE-T value of 301LN-2 alloy could be attributed to the nonhomogeneous nature of the passive film. The inhomogeneity within the film is a result of local defects, which weaken the chemical bonds and the film property. Lower value of CPE-T also implies the formation of more protective film on the electrode surface, indicating better stability of the passive film. Based on the above results, the impedance film resistance of higher N-containing alloys is better, but cold-rolled alloy shows poor passive film stability. Chou et al. (Ref 10) using impedance measurement has observed that the passive film stability of type 301L stainless steel was greatly affected by the N content. They demonstrate that the presence of N in type 301L stainless steel either inhibit the corrosion or assist the passivation processes. Similarly, in the present results, some correlation of N content with film stability has been observed. Based on the above results, some characteristic trends are visible depending on the metallurgical conditions and N content despite the scatter in alloy composition of the investigated alloys.

4. Conclusions

The evaluation of pitting corrosion and IGC resistance of AISI type 301LN stainless steels and its relation to phase changes induced by cold working and annealed conditions has been studied. The microstructure after sensitization heat treatment revealed insignificant $Cr_{23}C_6$ precipitation for both imported and indigenous materials. The negligible carbide precipitates is attributed to low C content and N that delay the onset of $Cr_{23}C_6$ precipitates. Furthermore, the bend test indicated no crack formation in all investigated alloys, thus revealing insignificant sensitization in the investigated alloys. The relative pitting corrosion resistance measured at different temperatures of 22 and 50 °C indicated pitting corrosion attack in all the alloys under accelerated 6% $FeCl_3$ test condition. However, the potentiodynamic anodic polarization results in 0.5 M NaCl solution revealed that pitting corrosion resistance of indigenous type 301LN stainless steels are better or equal to the imported grade type 301LN stainless steel in chloride media. The EIS results correlated well with the polarization results as indicated by higher film resistance for higher N-containing alloy and lower film stability for as-cold-rolled alloy. In cold-worked alloy, the formation of strain-induced martensite was detrimental to both pitting corrosion resistance and passive film stability.

Acknowledgments

The authors wish to thank SAIL, Salem Steel Plant, Salem, India for providing all the type 301LN stainless steels and Dr. S. Murugesan of Physical Metallurgy Division, IGCAR for the XRD measurement.

References

1. V.G. Gavriljuk and H. Berns, Eds., *High Nitrogen Steels (Structure, Properties, Manufacture, Applications)*, Springer-Verlag, Berlin, Germany, 1999, p 135–198
2. U. Kamachi Mudali and S. Ningshen, Corrosion Properties of Nitrogen Bearing Stainless Steels, *High Nitrogen and Stainless Steels—Manufacturing, Properties & Applications*, U. Kamachi Mudali and B. Raj, Ed., Narosa Publishing House, New Delhi and ASM International, The Materials Information Society, Materials Park, OH, 2004, p 133–181
3. J.W. Simmons, Overview: High-Nitrogen Alloying of Stainless Steels, *Mater. Sci. Eng. A*, 1996, **207**(2), p 159–169
4. V.G. Gavriljuk, Nitrogen in Iron and Steel, *ISIJ Inter.*, 1996, **36**(7), p 738–745
5. M.O. Speidel, Properties and Applications of High Nitrogen Steels: Austenites and Duplex, *Proceedings of International Conference on High Nitrogen Steels (HNS 88)*, J. Foct and A. Hendry, Ed., May 1988 (France), The Institute of Metals, London, 1989, p 92–96
6. A. Barbucci, M. Delucchi, M. Panizza, M. Sacco, and G. Cerisola, Electrochemical and Corrosion Behaviour of Cold Rolled AISI 301 in 1 M H_2SO_4, *J. Alloys Compd.*, 2001, **317–318**(60), p 7–611
7. S.D. Washko and G. Aggen, *Metals Handbook*, *Vol 1, Properties and Selection: Irons, Steels, and High-Performance Alloys*, 10th ed., ASM International, Materials Park, OH, 1990, p 841–907
8. P.H. Declety, Stainless Steel Railcars for Mass Transit Systems, *Stainless Steel Focus*, 1993, **82**, p 15–16
9. R.R. Gopal, Emerging Applications of Stainless Steel in India, *Miner. Met. Rev.*, 2005, **31**(5), p 69–71
10. S. Chou, M. Tsai, W. Tsai, and J. Lee, Effect of Nitrogen on the Electrochemical Behavior of 301LN Stainless Steel in H_2SO_4 Solutions, *Mater. Chem. Phys.*, 1997, **51**, p 97–107
11. V.F. Zackay, E.R. Parker, D. Fahr, and R. Busch, The Enhancement of Ductility in High-Strength Steels, *ASM Trans. Quart.*, 1967, **60**(2), p 252–259
12. S. Budano and G. Florio, Fatigue Behaviour of Austenitic Stainless Steel Sheets for Railcars, *Proceedings of the International Conference on Processes and Materials: Innovation Stainless Steel*, Vol 1, Oct 11-14, 1993 (Florence, Italy), p 1.277–1.284

13. G.L. Huang, D.K. Matlock, and G. Krauss, Martensite Formation, Strain rate Sensitivity, and Deformation Behavior of Type 304 Stainless Steel Sheet, *Metall. Trans. A*, 1989, **20**(7), p 1239–1246
14. T. Tanaka and K. Hoshino, New Developments in Stainless Steel Technology, Proceedings of the International Conference on Interface Migration and Control of Microstructure, Sept 17-21, 1984 (Detroit, MI), American Society of Metals, Metals Park, OH, p 129–137
15. "Standard Practices for Detecting Susceptibility to Intergranular Attack in Austenitic Stainless Steels." ASTM Practice A 262 Method, *Annual Book of ASTM Standards*, Vol 03.02, ASTM International, West Conshohocken, PA, 1994
16. "Standard Test Methods for Pitting and Crevice Corrosion Resistance of Stainless Steels and Related Alloys by Use of Ferric Chloride Solution." ASTM Standard Practice G 48, *Annual Book of ASTM Standards*, Vol 03.02, ASTM International, West Conshohocken, PA, 1994
17. U. Kamachi Mudali, R.K. Dayal, T.P.S. Gill, and J.B. Gnanamoorthy, Influence of Microstructure and Pitting Corrosion Resistance of Austenitic Welds Metals, *Werks. Korros.*, 1986, **37**, p 637–643
18. S. Ningshen, U. Kamachi Mudali, and R.K. Dayal, Electrolyte and Temperature Effects on Pitting Corrosion of Type 316LN Stainless Steels, *Br. Corros. J.*, 2001, **36**(1), p 36–41
19. J.R. Macdonald, Ed., *Impedance Spectroscopy—Emphasizing Solid Materials and Systems*, Chap. 1-4, Wiley, New York, 1987
20. J. Talonen, P. Aspegren, and H. Hänninen, Comparison of Different Methods for Measuring Strain Induced α-Martensite Content in Austenitic Steels, *Mater. Sci. Technol.*, 2004, **20**(12), p 1506–1512
21. V. Seetharaman and P. Krishnan, Influence of the Martensitic Transformation on the Deformation Behaviour of an AISI 316 Stainless Steel at Low Temperatures, *J. Mater. Sci.*, 1981, **16**(2), p 523–530
22. C.B. Post and W.S. Eberly, Stability of Austenite in Stainless Steels, *Trans. ASM*, 1946, **39**, p 868–890
23. M.R. Berrahmoune, S. Berveiller, K. Inal, and E. Patoor, Delayed Cracking in 301LN Austenitic Steel After Deep Drawing: Martensitic Transformation and Residual Stress Analysis, *Mater. Sci. Eng. A*, 2006, **438–440**, p 262–266
24. M.W. Bowkett, S.R. Keown, and D.R. Harries, Quench and Deformation-Induced Structures in Two Austenitic Stainless Steels, *Met. Sci.*, 1982, **16**(11), p 499–517
25. U. Kamachi Mudali, R.K. Dayal, J.B. Gnanamoorthy, and P. Rodriguez, Relationship Between Pitting and Intergranular Corrosion of Nitrogen-Bearing Austenitic Stainless Steels, *ISIJ Inter.*, 1996, **36**(7), p 799–806
26. U. Kamachi Mudali, R.K. Dayal, J.B. Gnanamoorthy, and P. Rodriquez, Influence of Thermal Aging on the Intergranular Corrosion Resistance of Types 304LN and 316LN Stainless Steels, *Metall. Mater. Trans. A*, 1996, **27**, p 2881–2887
27. Y.J. Oh and J.H. Hong, Nitrogen Effect on Precipitation and Sensitization in Cold-Worked Type 316L(N) Stainless Steels, *J. Nucl. Mater.*, 2000, **278**(2–3), p 242–250
28. T.A. Mozhi, A.T. Clark, W.B. Johnson, D.D. Macdonald, and K. Nishimoto, The Effect of Nitrogen on the Sensitization of AISI 304 Stainless Steel, *Corrosion*, 1985, **40**(10), p 555–559
29. N. Parvathavarthini and R.K. Dayal, Influence of Chemical Composition, Prior Deformation and Prolonged Thermal Aging on the Sensitization Characteristics of Austenitic Stainless Steels, *J. Nucl. Mater.*, 2002, **305**(2–3), p 209–219
30. A.S. Hamada, L.P. Karjalainen, and M.C. Somani, Electrochemical Corrosion Behaviour of a Novel Submicron-Grained Austenitic Stainless Steel in an Acidic NaCl Solution, *Mater. Sci. Eng. A*, 2006, **431**(1–2), p 211–217
31. Y. Kasuga, Change in Shape of a Cold Formed and Annealed Stainless Steel Sheet and Joining with use of this Change, *J. Mater. Process. Technol.*, 1996, **60**(1–4), p 233–238
32. B. Mazza, P. Pedeferri, A. Cigada, G.A. Mondara, G. Re, G. Taccani, and D. Wenger, Pitting Resistance of Cold-Worked Commercial Austenitic Stainless Steels in Solution Simulating Sea Water, *J. Electrochem. Soc.*, 1979, **126**(12), p 2075–2081
33. U. Kamachi Mudali, S. Ningshen, A.K. Tyagi, and R.K. Dayal, Influence of Metallurgical and Chemical Variables on the Pitting Corrosion Behaviour of Nitrogen-Bearing Austenitic Stainless Steels, *Mater. Sci. Forum*, 1999, **318–320**, p 495–502
34. U. Kamachi Mudali, P. Shankar, S. Ningshen, R.K. Dayal, H.S. Khatak, and B. Raj, On the Pitting Corrosion Resistance of Nitrogen Alloyed Cold Worked Austenitic Stainless Steels, *Corros. Sci.*, 2002, **44**(10), p 2183–2198
35. K. Elayaperumal, P.K. De, and J. Balachandra, Passivity of Type 304 Stainless Steel—Effect of Plastic Deformation, *Corrosion*, 1972, **28**(7), p 269–273
36. W.S. Li, N. Cui, and J.L. Luo, Pitting Initiation and Propagation of Hypoeutectoid Iron-Based Alloy with Inclusions of Martensite in Chloride-Containing Nitrite Solutions, *Electrochim. Acta*, 2004, **49**(9–10), p 1663–1672
37. S. Sunada, H. Maesato, Y. Yokio, H. Notota, and S. Sanuki, Effect of Deformation-Induced Martensite on Pitting Corrosion, *J. Jpn. Inst. Metals*, 1990, **54**, p 1078–1086
38. S. Ningshen, U. Kamachi Mudali, A. Amarendra, P. Gopalan, R.K. Dayal, and H.S. Khatak, Hydrogen Effects on the Passive Film Formation and Pitting Susceptibility of Nitrogen Containing Type 316L Stainless Steels, *Corros. Sci.*, 2006, **48**(5), p 1106–1121
39. C.-O.A. Olsson and D. Landolt, Passive Films on Stainless Steels—Chemistry, Structure and Growth, *Electrochim. Acta*, 2003, **48**(9), p 1093–1104